



ELSEVIER



Hepatobiliary Imaging in Liver-directed Treatments

Caren van Roekel, MD[#] Margot T.M. Reinders, MSc[#] Sandra van der Velden, MSc,
Marnix G.E.H. Lam, MD, PhD, and Manon N.G.J.A. Braat, MD

Hepatobiliary scintigraphy (HBS) is an emerging tool in the assessment of hepatic function. This nuclear imaging technique can be used to calculate both global and regional liver function. It has proven to be the most reliable way of assessing the distribution of liver function, especially in patients with impaired liver function due to, for example, cirrhosis or after chemotherapy. There are two types of tracers: Technetium-99m with a type of iminodiacetic acid and Technetium-99m galactosyl human serum albumin. The main indication for HBS is the assessment of the future liver remnant function in patients scheduled to undergo hemihepatectomy; to predict the risk of posthepatectomy liver failure. Another upcoming indication is the use of HBS in patients undergoing radioembolization.

Semin Nucl Med 49:227-236 © 2019 Elsevier Inc. All rights reserved.

Introduction

Hepatobiliary scintigraphy (HBS) with ^{99m}Tc was first described in 1975 by Harvey et al.¹ This imaging technique is a promising tool in predicting the future remnant liver function (FRL-F) in patients who undergo liver treatment, regardless of underlying liver disease.² It is used for direct calculation of global and regional liver function. Currently, there are two types of tracers: Technetium-99m galactosyl human

serum albumin (^{99m}Tc GSA) and Technetium-99m with a type of iminodiacetic acid (IDA) (^{99m}Tc IDA).

In the past decades, liver-directed treatments for primary and secondary liver tumors have increased. New techniques were developed—such as laparoscopic liver surgery, radio-frequency ablation, microwave ablation, radioembolization, stereotactic radiation therapy, transarterial chemo-embolization—and perfected. In larger liver directed treatments, that is, (extended) hemihepatectomies and (bi)lobar radioembolization, (lethal) liver failure can develop. Estimation of the function of the liver remnant is therefore indispensable, especially in patients with hepatic comorbidity and resultant diminished liver regeneration capacity.

Abbreviations: ALBI, albumin-bilirubin; ALP, alkaline phosphatase; ALT, alanine aminotransferase; AST, aspartate aminotransferase; ATP, adenosine triphosphate; BSA, body surface area; Clr, clearance rate; CPT, Child-Pugh-Turcotte; FOV, field of view; FRL-F, future remnant liver function; FRL-V, future remnant liver volume; Gd-EOB-DTPA, gadolinium ethoxybenzyl diethylenetriamine pentaacetic acid; GGT, γ -glutamyltransferase; HBS, hepatobiliary scintigraphy; ICG, indocyanine green; INR, international normalized ratio; LDH, lactate dehydrogenase; MDRP2, multidrug resistance protein 2; MELD, Model for End-Stage Liver Disease; NTCP, sodium taurocholate cotransporting polypeptide; OATP, organic anion transporting polypeptide; PHLF, posthepatectomy liver failure; PRI, predictive residual index; PVE, portal vein embolization; REILD, radioembolization-induced liver disease; ROI, region of interest; sFRL-V, standardized future remnant liver volume; ^{99m}Tc GSA, Technetium-99m galactosyl human serum albumin; ^{99m}Tc IDA, Technetium-99m iminodiacetic acid

Department of Radiology and Nuclear Medicine, University Medical Center Utrecht (UMCU), Utrecht, the Netherlands.

Address reprint requests to Manon N.G.J.A. Braat, University Medical Center Utrecht, Heidelberglaan 100, 3584 CX, Utrecht, The Netherlands.

E-mail: M.N.G.Braat-3@umcutrecht.nl

[#]Contributed equally.

Hepatic Anatomy and Physiology

The liver is the largest gland of the human body. Anatomically, it is separated into a right and a left lobe and it can be further divided into eight separate functioning segments, based on Couinaud³ (Fig. 1). The blood supply of the liver is twofold: it receives blood from the portal vein ($\approx 75\%$) and the hepatic artery ($\approx 25\%$). Blood exits the liver through the hepatic veins.

The liver parenchyma consists of plates of hepatocytes that are surrounded by reticuloendothelial cells. Very small vascular spaces, the sinusoids, separate the diverse plates and drain into central veins. Portal triads are structures containing a portal venule, hepatic arteriole and a bile canaliculus and surround the hepatic plates with their central veins (Fig. 2).

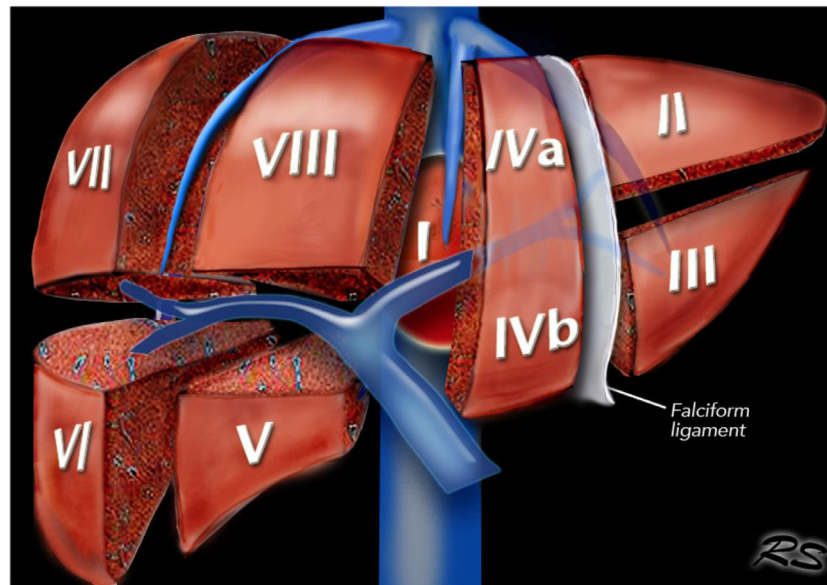


Figure 1 Segmental hepatic anatomy according to Couinaud. Reprinted with permission of Robin Smithuis, MD, from radiologyassistant.com.

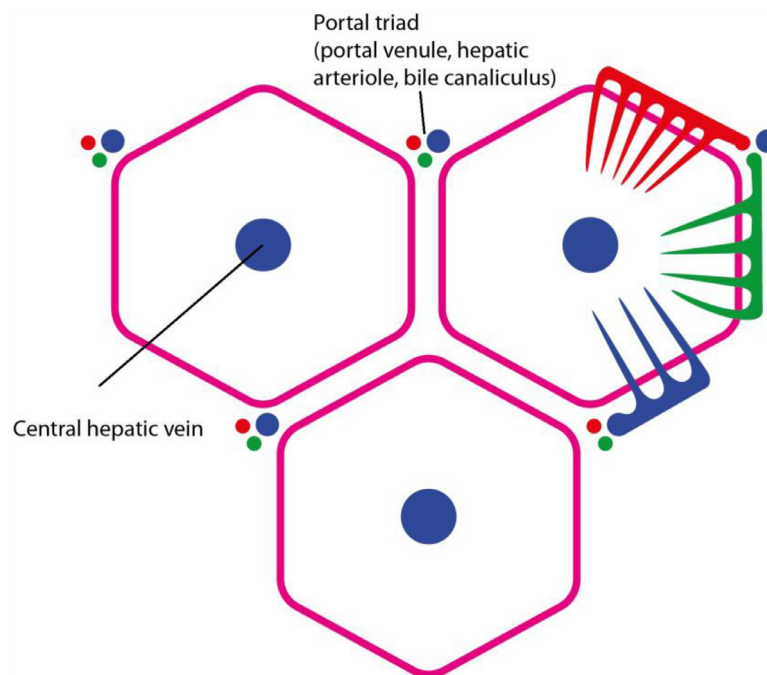


Figure 2 Hexagon structure of hepatocytes with portal triad.

Hepatocytes have three sides: the apical surface, the basolateral surface, and the lateral domain. Uptake of proteins and molecules from the bloodstream and secretion of particles into the bloodstream takes place at the basolateral surface, whereas bile transport and excretion occurs at the apical surface.⁴

This unique architecture of the liver parenchyma enables the liver to fulfill diverse functions, including receptor-mediated uptake and transport of molecules. A major excretory function of the liver is bile production. Hepatocytes synthesize bile acids from cholesterol at a rate of approximately 200-400 mg/day. Conjugated bile, when a bile

molecule is linked to glycine or taurine, is transported out of the hepatocyte into the canaliculus by transporters of the adenosine triphosphate binding family, such as multidrug resistance protein 2 (MDRP2).⁴ From the canaliculi, it is transferred to bile ductules and then further transported to the biliary tree Fig. 3.

Liver Function Assessment

Several liver-related biochemical substances can be measured in the blood plasma to estimate global hepatic function, such

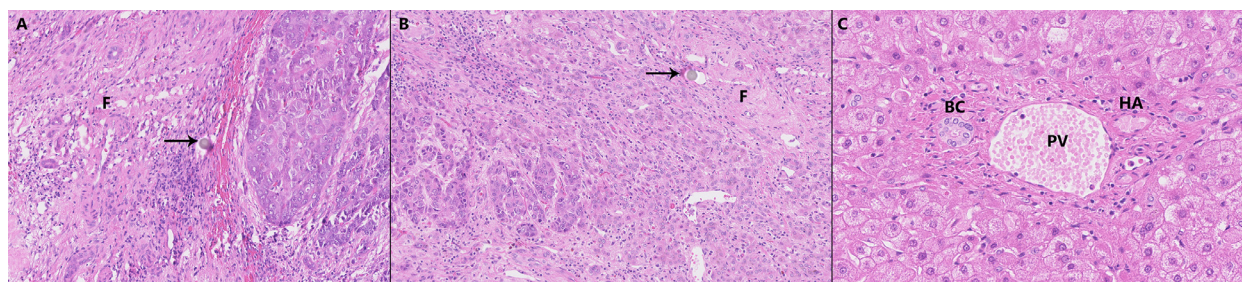


Figure 3 This figure shows histological images of the pathological tissue of an HCC patient that was taken after radio-embolization. A microsphere can be seen (A, B) (black arrows), next to fibrosis (F). (C) The portal triad with the PV in the center of the image, an HA on the right and BC on the left. HCC, hepatocellular carcinoma; PV, portal venule; HA, hepatic arteriole; BC, bile canaliculus.

as alanine aminotransferase, aspartate aminotransferase, lactate dehydrogenase, γ -glutamyltransferase), alkaline phosphatase, albumin and total and conjugated bilirubin.

However, most of these blood assays are poor representatives of hepatic function. Alanine aminotransferase and aspartate aminotransferase, for example, are markers of hepatocyte injury or necrosis and not an estimate of hepatic function. Likewise, γ -glutamyltransferase and alkaline phosphatase are indicators of cholestasis, rather than hepatic function. Conjugated bilirubin however is related to uptake, conjugation and excretion functions of the liver and could therefore be a valuable marker of hepatic function. Yet, a high plasma bilirubin can be caused by hemolysis or posthepatic biliary obstruction without impairment of hepatocyte function.⁵ Thus, blood assays alone are no absolute measurement tool for hepatic function. Even clinical scoring systems based on these blood parameters are of limited use in the evaluation of (regional) liver function. The clinical scoring systems that are currently most widely used are the Model for End-Stage Liver Disease (MELD) score, the albumin-bilirubin grade and the Child-Pugh classification. The MELD score is a validated metric to describe the severity of liver disease. It was originally developed to predict survival in patients undergoing placement of intrahepatic portosystemic shunts, but it is now mostly used for allocation of organs for liver transplantation as it can distinguish patients according to their mortality risk. The MELD score consists of the international normalized ratio (INR), creatinine, and bilirubin. A major strength of the MELD score is that it is widely validated and that it is based on objective values. However, an important drawback of this score is that it cannot predict mortality after elective liver resection.⁶ The albumin-bilirubin grade is a relatively new measure, developed to evaluate liver function in patients with hepatocellular carcinoma (HCC). It is categorized into three different grades, based on serum bilirubin and albumin. It is an accurate predictor of the risk of posthepatectomy liver failure (PHLF) and survival in patients undergoing liver resection.^{7,8} The Child-Pugh-Turcotte is based on the following parameters: ascites, encephalopathy, bilirubin, albumin, and INR. It is used to select patients with HCC and cirrhosis for transplantation or resection. A limitation of this score is the subjectivity of the parameters ascites and encephalopathy.⁹ A major limitation of all three scoring systems is their inability to define regional

liver function. Indocyanine green (ICG) clearance tests can be used to measure functional hepatocyte mass. ICG is a tricarbo-cyanine dye.¹⁰ After uptake into the hepatocytes it is excreted by the MDRP2 transporter (similar to bilirubin) into the bile, but without intrahepatic conjugation. Therefore, the clearance rate in the blood, after peripheral injection, reflects the liver's capacity to transport organic anions and metabolize drugs, and thus provides an indirect measurement of global liver function.¹¹ Several repeated blood samples are required to evaluate the clearance rate in the peripheral blood, for example, before and at 5, 10, 15, and 20 minutes after ICG injection.¹⁰ ICG tests can assess global liver function, but not the distribution among liver segments. Other drawbacks are that the ICG clearance rate is influenced by hepatic blood flow variations and hyperbilirubinemia.^{5,12}

Currently though, the most often used method for evaluating whether patients are suitable candidates for hepatic resection is not based on functional measurements, but on CT-or MRI-based volumetry. The future remnant liver volume (FRL-V) can be accurately estimated using CT or MRI.^{13,14} The cut-off value for resection in patients with noncompromised liver tissue is an FRL-V of at least 30%. For patients with compromised liver tissue, for example, due to cirrhosis, the cut-off value is 50%.¹⁵ Still, the segmental distribution of the liver function and the extent of the regenerative impairment remain unknown. Moreover, prior to the liver-directed therapy, the existence of hepatic disease is not always known, thus introducing unnecessary risk of liver failure.

Hepatobiliary Scintigraphy

HBS is used for direct calculation of global and regional liver function. Both tracers, ^{99m}Tc GSA and ^{99m}Tc IDA, will be discussed.

HBS With IDA Agents

There are three types of IDA radiopharmaceuticals that are used for hepatic function evaluation: ^{99m}Tc lidofenin (HIDA), ^{99m}Tc disofenin Technetium-99m disofenin

iminodiacetic acid (DISIDA), and ^{99m}Tc mebrofenin (BrIDA).¹⁶ ^{99m}Tc mebrofenin has the highest hepatic uptake—thus most strongly resists competition with bilirubin in hyperbilirubinemia—and renal excretion is minimal.^{5,12,16}

IDA binds to plasma carrier proteins, mainly albumin. It is transported into the hepatocyte via the organic anion transporting polypeptide receptor. After uptake in the hepatocyte, IDA follows the bilirubin pathway and is excreted into the bile canaliculi by MDRP2 transporters^{16,17} without any biotransformation.¹²

Calculation and Acquisition

HBS consists of a multi-phase scanning protocol. Patients are scanned in the supine position and the field of view should include the aortic notch and the entire liver. First, immediately after intravenous injection of the IDA, dynamic anterior and posterior images are acquired (36 frames: 10 s/frame; 128×128 matrix; energy window: $140 \text{ keV} \pm 7.5\%$). These images are used to calculate the total hepatic uptake rate. Second, a fast SPECT/CT is acquired (60 projections; 8 s/projection; 128×128 matrix; energy window: $140 \text{ keV} \pm 7.5\%$). This acquisition is centered on the peak of the hepatic time-activity curve and can be used to assess regional hepatic uptake. Third, a second dynamic acquisition with similar parameters as during the first phase is acquired, but this time only 15 frames of 60 s/frame are acquired. This last acquisition serves to evaluate biliary excretion. Finally a low dose CT is acquired for attenuation correction and anatomical reference.

In 1996, Ekman et al. developed a method to calculate the total liver function from the dynamic images of the first phase, which is now widely used in clinical practice.¹⁸ To account for attenuation effects, calculations are performed on a geometric mean (G_{mean}) dataset, which is formed by taking the square root of the product of the anterior and posterior projection images.¹³ First, several regions of interest are drawn: one over the liver, another over part of the heart and the large vessels, and a third region of interest over the entire field of view. The clearance rate of the liver can then be estimated from the corresponding time-activity curves using the following formula:

$$\text{LCI} = \frac{\text{LCI}}{V} = \frac{L(t_2) - L(t_1)}{A(t_1) \int_{t_1}^{t_2} C_{\text{norm}}(t) dt}$$

In this formula, the liver clearance rate is defined as the fraction of IDA that is cleared per time unit from the blood pool, with V the volume of the blood pool in (mL). $L(t)$ is the amount of activity that has accumulated in the liver at time t ; t_1 and t_2 are the beginning and end time on the time-activity curves used in the calculation. A relatively strict time frame of 150-350 seconds after injection is used, to ensure that calculations are made during a phase of homogeneous distribution of the IDA in the blood pool. $A(t_1)$ is the total amount of circulating activity at time

t_1 and $C_{\text{norm}}(t)$ is $A(t)$ normalized to unity at time t_1 .¹⁹ To compensate for variations in individual metabolic needs, this clearance rate is divided by the body surface area (m^2). Hepatic uptake rate is thus expressed in $[\%/\text{min}/\text{m}^2]$.^{5,14} Segmental liver function is calculated from the SPECT/CT using the total liver function as a reference. The number of counts in the “segment of interest” is divided by the total liver counts and this percentage reflects the segmental function relative to the total liver function.¹³

Surgery

HBS can be used to predict postoperative liver failure in patients planned to undergo liver resection. De Graaf et al. examined the accuracy of HBS in the prediction of postoperative liver failure after (extended) hemihepatectomy in high-risk patients ($n = 55$). CT volumetry was compared with ^{99m}Tc mebrofenin HBS. In patients with normal livers, the FRL-V correlated well with FRL-F, contrary to patients with a compromised liver. Nine of 55 patients developed PHLF. Based on receiver operating characteristic (ROC)-analysis, a cutoff value of $2.69\%/\text{min}/\text{m}^2$ was identified to estimate the risk of postoperative liver failure (sensitivity 89%/specificity 87%), regardless of underlying liver disease. This cutoff value was found to be a better predictor of postoperative liver failure than FRL-V. In this specific study, only planar HBS images were used, without an accompanying low-dose CT. The CT volumetry images were used as a guideline to delineate the FRL on the HBS images. Using the current techniques for HBS with a SPECT/CT, regional differences can be estimated more accurately.¹³

In a more recent study, Chapelle et al. investigated the value of ^{99m}Tc mebrofenin HBS combined with volumetry in the prediction of PHLF in a cohort of 88 patients who underwent hemihepatectomy. FRL-F was calculated as: $\text{FRL-V}/\text{nontumor total liver volume} \times \text{total liver function}$ as measured on HBS. PHLF was diagnosed according to the international criteria; that is, $\text{INR} > 1.5$ and serum bilirubin $> 1.2 \text{ mg/dL}$ ($21 \mu\text{mol/L}$) on day 5 postsurgery.²⁰ Twelve patients developed PHLF. Liver function estimation by ^{99m}Tc mebrofenin HBS was found to be a significant predictive factor of PHLF in this patient cohort, with a cut-off value of $2.3\%/\text{min}/\text{m}^2$ and a positive predictive value of 92%, in contrast with FRL-V.¹⁴ Given the calculation method of the FRL-F in this study, segmental differences in liver function were not taken into account. Furthermore, the earlier study by de Graaf et al. described a significant underestimation of the actual postoperative liver remnant function using this method; probably explaining the lower cut-off value in this study.¹³

To improve the success rate of major liver surgery, preoperative portal vein embolization (PVE) was developed in Japan around 1986. PVE induces hepatic (lobar) atrophy through embolization of the portal branches of the diseased liver lobe. This results in an increase of the FRL-V and FRL-F²¹ (Fig. 4). Yet, Future remnant liver - function (FLR-F) increases significantly more than FLR-V post-PVE.

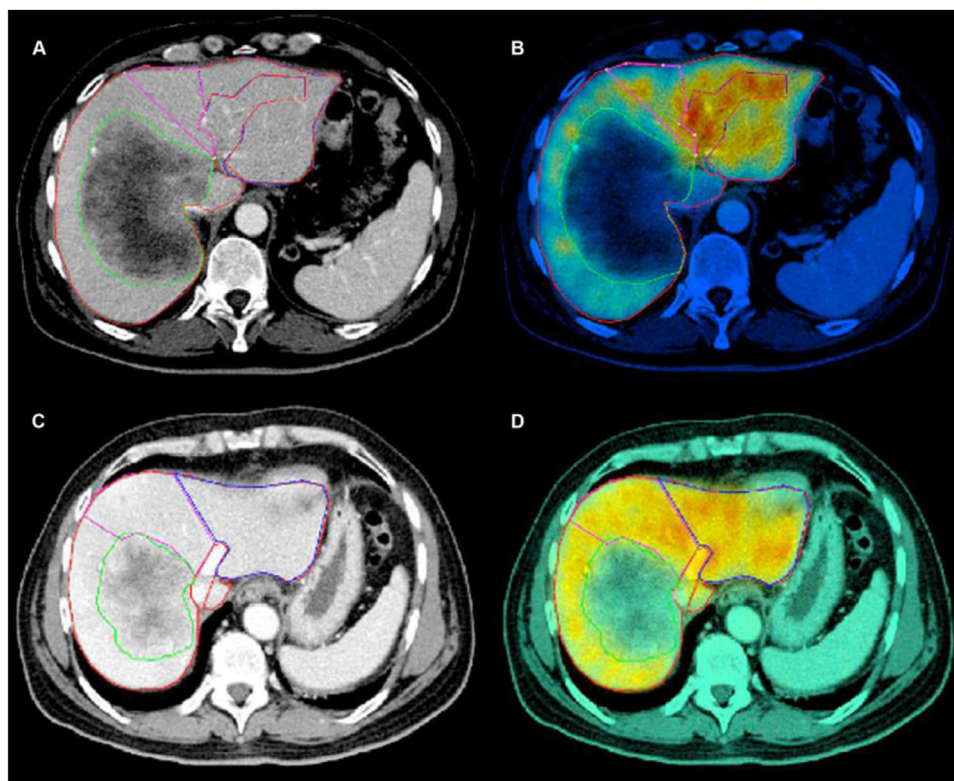


Figure 4 This figure shows the ^{99m}Tc mebrofenin SPECT/CT images of a patient with a large cholangiocarcinoma in the right hemiliver. (A, B) Show the inhomogeneous hepatic function before right PVE. The total liver function was $6.3\%/ \text{min}/\text{m}^2$. Segmental function of segments 2-3 was $1.8\%/ \text{min}/\text{m}^2$. (C, D) Show the hepatic function 1 month after PVE. The tumor has shrunk and there was an increase in total liver function to $8.8\%/ \text{min}/\text{m}^2$. The FLR-F of segments 2 and 3 was $2.7\%/ \text{min}/\text{m}^2$, which was sufficient for right hemihepatectomy. PVE, portal vein embolization, FLR-F Future remnant liver - function.

In practice, this may result in shorter intervals between PVE and surgery than suggested by volumetric parameters.²¹ Cieślak et al. showed an increase in mean FLR-F after PVE of $1.80\%/ \text{min}/\text{m}^2$ to $2.89\% / \text{min}/\text{m}^2$ in a study of 63 patients. Furthermore, they noted that the pre-PVE FRL-F can be predictive for the development of adequate function increase, with a pre-PVE FRL-F cut-off value of $1.72\%/ \text{min}/\text{m}^2$ for chemo-naïve patients and $1.92\%/ \text{min}/\text{m}^2$ for patients who received chemotherapy.²²

If PVE is expected to be insufficient, patients may benefit from associating liver partition and portal vein ligation for staged hepatectomy (ALPPS). ALPPS accomplishes a stronger and much faster hypertrophy response by in situ dividing of the liver tissue and adjuvant portal vein ligation.^{22,23} However, when performing ALPPS, the poor correlation between liver volume and function should be taken into account as well. Olthof et al. showed that FRL-V increased with a median of 78% during a median of 8 days after stage 1, while FRL-F only increased with a median of 29% after 7 days, in 27 patients with both measurements.²⁴ Interestingly, this is contrary to the findings of De Graaf et al., who found that after PVE, there was a higher increase in FRL-F than in FRL-V.²¹ Olthof et al. state that this discrepancy may be due to a fast hypertrophied, but functionally immature FRL and performing surgery based on volumetric measures alone may lead to a high incidence of PHLF.²⁴ Integration of the complex surgical strategies and preoperative (volumetric and/or

functional) liver tests are paramount to good patient selection. Therefore, hepatologists, surgeons, radiologists, and nuclear physicians should work in close collaboration.^{25,26}

Radioembolization

Though radioembolization initially was only considered a treatment option for patients with primary or secondary liver tumors in a palliative stage, it is currently emerging as a bridge to surgery or transplant. Microspheres embedded with the radio-isotope yttrium-90 (^{90}Y) or holmium-166 (^{166}Ho) are injected into the hepatic artery, resulting in microsphere deposition in the tumor arterioles and tumor radiation. However, part of the microspheres are deposited in normal portal triads. Inadvertent radiation of the nontarget liver tissue may lead to radioembolization-induced liver disease (REILD). REILD is defined as: “a symptomatic post-radioembolization deterioration in the ability of the liver to maintain its (normal or pre-procedural) synthetic, excretory, and detoxifying functions. It is characterized by jaundice and the development of, or increase in, ascites, hyperbilirubinemia, and hypoalbuminemia, developing at least 2 weeks to 4 months after radioembolization, in the absence of tumor progression or biliary obstruction.” And, although the aim of treatment with

radioembolization is to spare the healthy liver tissue, the reported incidence of lethal REILD is still up to 5%.²⁷

Currently, eligibility for radioembolization is based on several factors, including multiple laboratory values and the presence of ascites, as proxies for liver function. Although it is difficult to predict the FRL-F after radioembolization, due to the heterogeneity of the absorbed dose distribution, HBS could be used to tailor treatment and retreatments, thus to avoid REILD.

The literature on the role of HBS in radioembolization is scarce, only five cases have been described.^{11,28} In these cases, a deterioration of the total liver function was seen after treatment. In two of these cases, only the right liver lobe was treated and an increase in function of the left liver lobe, as well as hypertrophy, was seen after treatment.^{11,28} Figure 5 shows the case of a 74-year-old male with the development of REILD after right lobar radioembolization.

Naturally, the prediction of the FRL-F before radioembolization is more difficult than before surgery. Due to heterogeneous dose distribution (and resulting liver damage),^{29,30} the function decline is not absolute and the treated lobe can retain function, which is of value in cases without subsequent surgery. Regional assessment of liver function before radioembolization with HBS might be used to adapt treatment strategy in patients with impaired liver function, for

example, to perform sequential lobar treatment instead of whole liver treatment. A threshold for the remnant function of the untreated lobe still has to be determined.

Fortunately, several studies on hypertrophy after radioembolization—measured by CT volumetry—exist. Similar to PVE and ALPPS, radioembolization induces hypertrophy of the nontreated lobes, with hypertrophy percentages of 26%-47% occurring 44 days until as long as 9 months after treatment.³¹ However, hypertrophy generally takes much more time to occur than after PVE or ALPPS.³¹⁻³⁵ A prospective study on patients undergoing unilobar radioembolization for HCC (n = 24) was conducted by Teo et al. to assess early hypertrophy of the untreated liver lobe. A median hypertrophy of the untreated lobe of 3% (range: -12% to 42%) and 9% (range -12% to 179%), at 4-6 weeks and 8-12 weeks after radioembolization, respectively. There were no predictive factors for the rate of hypertrophy, nor was a correlation found between absorbed radiation dose and hypertrophy rate.³² In another retrospective study the median degree of hypertrophy was 4.2% (range 0.8%-12.3%) at 1 month, 7.5% (range 0.4%-25.9%) at 3 months and 11.5% (range 1.6%-27.3%) at 6 months.³⁶ Moreover, patients with a baseline Future remnant liver (FLR) of <20% of the entire volume never reached an FLR volume \geq 40%.³⁶ The latter finding is important for the possible role of

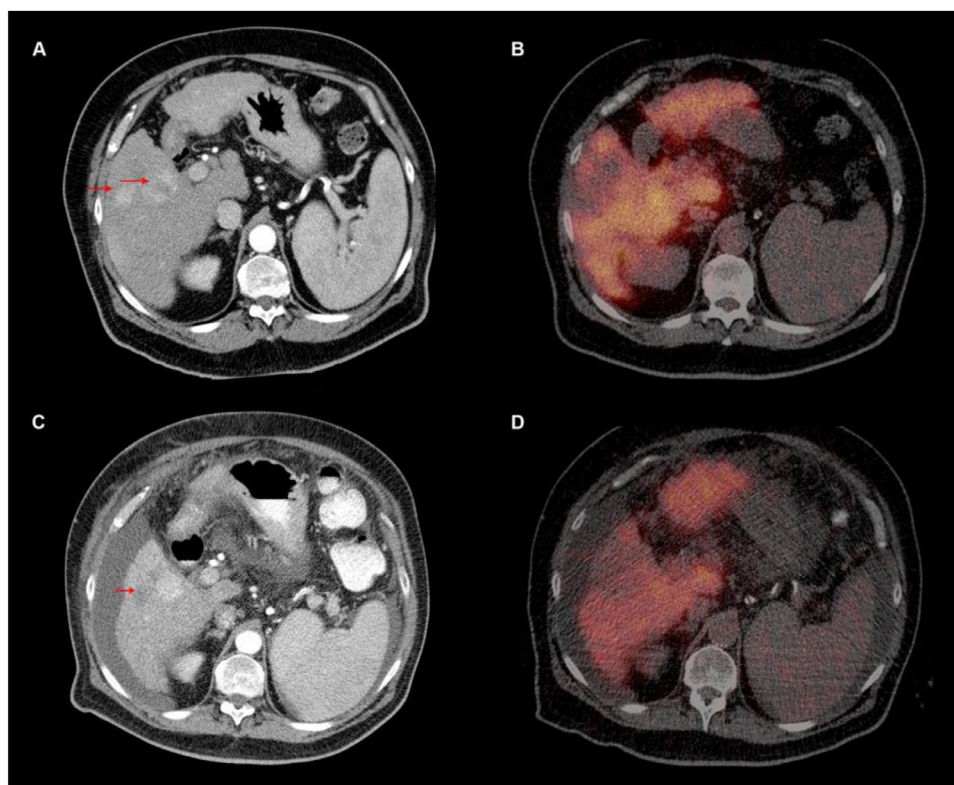


Figure 5 (A, B) Show the axial CT and corresponding fused HBS SPECT/CT images before treatment with radioembolization, with a cirrhotic liver with 2 hypervascular HCC lesions in segment 5 (“cold spots”) (red arrows). (C, D) Show necrosis of the lateral lesion in segment 5 (red arrow), but also the development of ascites 3 months after treatment with radioembolization of the right liver lobe. On the fused images a diminished uptake of ^{99m}Tc mebrofenin is seen. His total liver function declined from 3.0% to 2.4%/min/m². HBS, hepatobiliary scintigraphy; HCC, hepatocellular carcinoma.

radioembolization as bridge to surgery. Given the unknown FRL-F in these patients and the poor correlation of FRL-V and FRL-F in compromised livers, these patients might benefit from HBS instead of volumetry.

Although the hypertrophy rate is less than after PVE or ALPSS, radioembolization not only induces hypertrophy but has a simultaneous antitumor effect. A number of patients will not be operated upon due to tumor progression in the treated or nontreated lobe. This tumor progression is an aspect that has received too little attention, but in fact is fairly common. In the study of Teo et al., 5/24 patients developed new lesions in the untreated liver lobe.³² Likewise, in the study of Vouche et al. 17/83 patients developed new lesions in the left lobe after right radiation lobectomy.³⁷ Nonetheless, in a study on PVE 14/63 patients were excluded from resection due to new lesions or progression in the embolized lobe. The prolonged interval between radioembolization and surgery (the so-called “test-of-time,” due to the slower rate of hypertrophy) compared to PVE might allow us to improve surgical patient selection by unveiling subclinical FRL metastases and tumors with dismal biological behavior. And in case of inadequate FLR-hypertrophy after radioembolization, subsequent PVE remains a possibility.³⁸

Figure 6 shows a case of a patient with colorectal carcinoma liver metastases. She was treated with radiation lobectomy of segments 5-8. An increase of the FLR-V was seen, and an increase of the FLR-F was also confirmed by HBS.

In our center, the value of HBS in radioembolization treatments is evaluated in an ongoing study: the Holmium-166 radioembolization in HCC (HEPAR Primary) study (clinicaltrials.gov identifier [NCT03379844](https://clinicaltrials.gov/ct2/show/study/NCT03379844)). In this study, patients with HCC are treated with radioembolization using holmium-166 microspheres (QuiremSpheres, Quirem). Before and after treatment, their liver function is estimated using HBS with ^{99m}Tc mebrofenin.

Limitations

Since IDA follows the bilirubin pathway in the liver, there is competition with bilirubin. In patients with hyperbilirubinemia, receptor uptake can be hampered, leading to suboptimal liver function assessment. In patients with hyperbilirubinemia, HBS may underestimate liver function.³⁹ This also applies for hypoalbuminemia. Since albumin is the main plasma carrier of IDA, liver function may be underestimated in patients with hypoalbuminemia. In liver disease, hyperbilirubinemia and hypoalbuminemia are often present, consistent with the decrease in liver function. Other causes of hyperbilirubinemia and hypoalbuminemia should be corrected for to be able to produce a representative HIDA scintigraphy.¹⁶

Another limitation of HBS is its diagnostic value in the differentiation between allograft rejection after hepatic transplantation and biliary cholestasis. In an evaluation of 36 patients with a total of 76 ^{99m}Tc DISIDA hepatic scintigraphies, a normal uptake was found on HBS in six patients with rejection.^{40,41}

In selected cases of well-differentiated HCC, the tumor will show uptake of IDA. Though not a limitation of HBS in itself, this tumor uptake should be excluded using the SPECT and anatomical reference CT, as it does not represent actual functional liver. Figure 7 shows an example of a patient with an HCC with IDA uptake.

HBS with GSA

^{99m}Tc GSA is only commercially available in Japan and a known alternative for ^{99m}Tc mebrofenin in HBS. The level of the asialoglycoprotein receptor in hepatocyte membranes of mammals, for which ^{99m}Tc GSA has affinity, is decreased in patients with liver disease. Its accuracy was validated by comparing it with conventional liver function tests, such as Child-Pugh classification, cholinesterase level, and ICG clearance (gold standard). ICG clearance rate at 15 minutes and liver activity at 15 minutes (based on ^{99m}Tc GSA scintigraphy) were examined by Nanashima et al. in 2003 in 140 patients with or without underlying liver disease who underwent hepatectomy. The test results were significantly correlated and demonstrated that ^{99m}Tc GSA scintigraphy is a useful tool in indicating hepatectomy and predicting patient outcome.⁴²

Nishiyama et al. looked at the usefulness of a predictive residual index (PRI) for ^{99m}Tc GSA, as based on dynamic liver imaging. It turned out that a PRI of 0.4 or higher would give a low probability of PHLF in liver cancer patients with both metastatic and primary liver tumors. Furthermore, the functional liver volume and PRI increased when PVE was performed before liver surgery.⁴³ This was confirmed by the study of Nanashima et al., using both CT volumetry and ^{99m}Tc GSA scintigraphy.⁴⁴ However, increase in volume may not resemble increase in functional liver tissue, as Kono et al. found no correlation between observed FRL-V and maximum removal rate of the radiopharmakon in patients who underwent PVE before liver surgery.⁴⁵ This emphasizes the importance of FRL-F.

Future Developments

A newly developed technique is the use of contrast-enhanced MRI with Gadolinium ethoxybenzyl diethylenetriamine pentaacetic acid (Gd-EOB-DTPA; Primovist, or Eovist) for the evaluation of liver function. The pathway of Gd-EOB through the hepatocytes is identical to the uptake and clearance of IDA agents. The parenchymal enhancement over time can be used to estimate hepatic function: the contrast agent is taken up only by the hepatocytes and the increase in signal intensity of the liver parenchyma can be used to evaluate its integrity.⁴⁶ Furthermore, MRI offers a high spatial and temporal resolution. Various studies have shown a high correlation between ICG tests and Gd-EOB-MRI liver function indices.^{47,48} A prospective study of Geisel et al. in patients undergoing PVE showed that Gd-EOB-MRI may be used to evaluate the functional increase of the FLR.⁴⁹

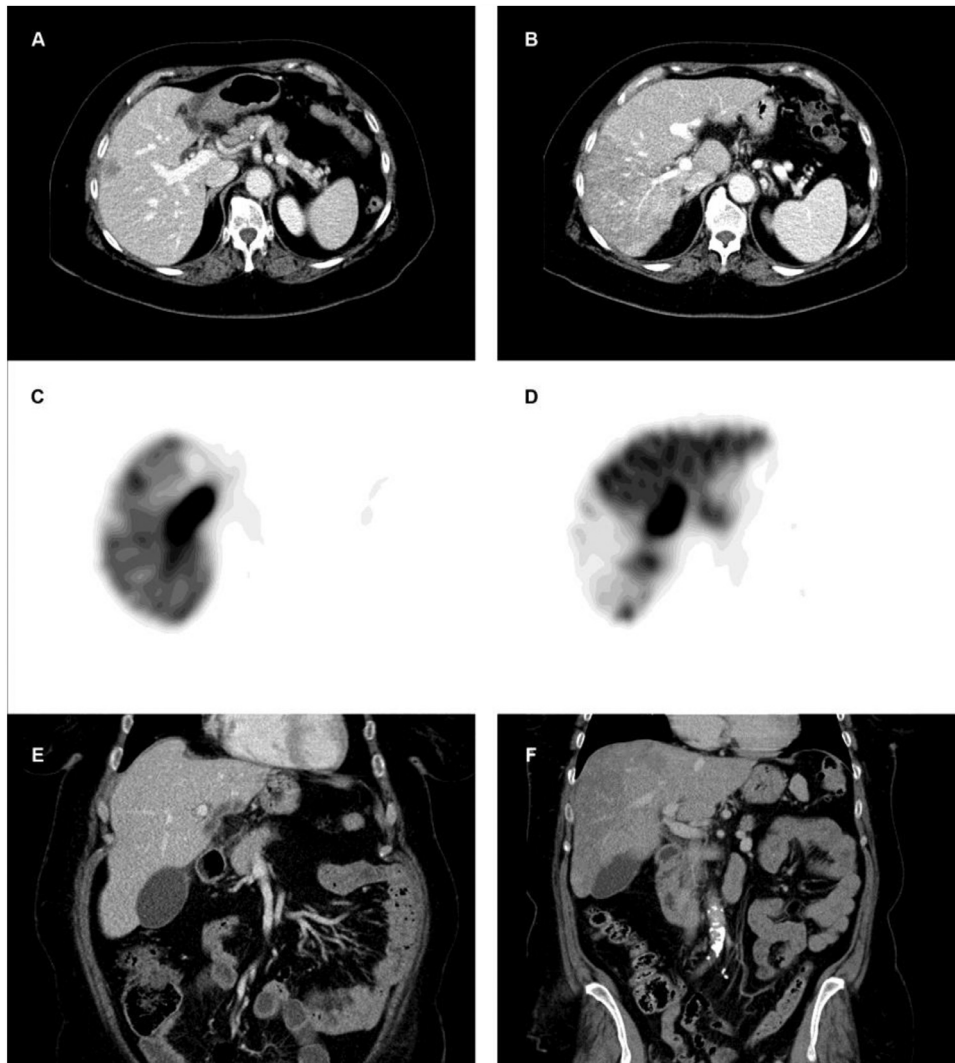


Figure 6 Case of a patient with colorectal liver metastases. (A, E) Show CT images of the liver in axial and coronal direction before radiation lobectomy. (B, F) Show CT images of the liver in axial and coronal direction 3 months after radiation lobectomy. Clear radiation damage (hypodense change of the liver parenchyma on CT) is seen in the treated right lobe (B). (C, D) Show the HBS images, with an atrophied right liver lobe and increase of function of the left liver lobe after radiation lobectomy (D). Before radiation lobectomy, the FLR-V (segments 1-4) was 523 cc, with a function of 1.99%/min/m². The volume of segments 5-8 was 1571 cc, with a function of 6.66%/min/m². The patient was treated with an aimed absorbed dose of 120 Gy in segments 5-8 (TheraSphere, BTG). After radiation lobectomy, the FLR-V increased to 1013 cc with a function of 4.0%/min/m²; note the hypertrophy of the segment 2 and 3 on the coronal CT reconstruction (E, F). The volume of the treated segments had decreased to 737 cc with a function of 1.2%/min/m².



Figure 7 (A) Shows the early arterial phase of a contrast-enhanced CT of a patient with a large central HCC. (B) Shows clear wash-out of the tumor in the late venous phase. In (C), there is heterogeneous uptake of ^{99m}Tc mebrofenin in the tumor.

Conclusion

Though first described in 1975, only in the last years HBS is gaining popularity as a tool to evaluate liver function. HBS outperforms CT volumetry for the prediction of liver failure following hepatic resections. Its value in other liver directed therapies is promising, but necessitates further investigation.

Acknowledgments

We would like to thank our colleagues from University Medical Center Utrecht: Miangela M. Laclé, MD, PhD from the Pathology department of the Division of Laboratory and Pharmacy for her support on the histology images and Chris van Kesteren from the Multimedia department of the Imaging Division for his support with the schematic figure.

References

- Harvey E, Loberg M, Cooper M: Tc-99m-HIDA: A new radiopharmaceutical for hepato-biliary imaging (abstract). *J Nucl Med* 16:533, 1975
- Hoekstra LT, de Graaf W, Nibourg GA, et al: Physiological and biochemical basis of clinical liver function tests: A review. *Ann Surg* 257:27-36, 2013
- Couinaud C: *Le foie. Etudes Anatomiques et Chirurgicales*. Paris: Masson, 1957
- Khalili M, Burman B: *Liver Disease. Pathophysiology of Disease: An Introduction to Clinical Medicine*. (7th ed). McGraw-Hill Education, 2014
- Bennink RJ, Tulchinsky M, de Graaf W, et al: Liver function testing with nuclear medicine techniques is coming of age. *Semin Nucl Med* 42:124-137, 2012
- Kamath PS, Kim WR: The model for end-stage liver disease (MELD). *Hepatology* 45:797-805, 2007
- Chan AW, Kumada T, Toyoda H, et al: Integration of albumin-bilirubin (ALBI) score into Barcelona Clinic Liver Cancer (BCLC) system for hepatocellular carcinoma. *J Gastroenterol Hepatol* 31:1300-1306, 2016
- Zhang ZQ, Xiong L, Zhou JJ, et al: Ability of the ALBI grade to predict posthepatectomy liver failure and long-term survival after liver resection for different BCLC stages of HCC. *World J Surg Oncol* 16:208, 2018
- Durand F, Valla D: Assessment of the prognosis of cirrhosis: Child-Pugh versus MELD. *J Hepatol* 42(Suppl):S100-S107, 2005
- Erdogan D, Heijnen BH, Bennink RJ, et al: Preoperative assessment of liver function: a comparison of 99mTc-Mebrofenin scintigraphy with indocyanine green clearance test. *Liver Int* 24:117-123, 2004
- Bennink RJ, Cieslak KP, van Delden OM, et al: Monitoring of total and regional liver function after SIRT. *Front Oncol* 4:152, 2014
- Bennink RJ, Dinant S, Erdogan D, et al: Preoperative assessment of post-operative remnant liver function Using hepatobiliary scintigraphy. *J Nucl Med* 45:965-971, 2004
- De Graaf W, van Lienden KP, van Gulik TM, et al: (99m)Tc-mebrofenin hepatobiliary scintigraphy with SPECT for the assessment of hepatic function and liver functional volume before partial hepatectomy. *J Nucl Med* 51:229-236, 2010
- Chapelle T, Op De Beeck B, Huyghe I, et al: Future remnant liver function estimated by combining liver volumetry on magnetic resonance imaging with total liver function on (99m)Tc-mebrofenin hepatobiliary scintigraphy: Can this tool predict post-hepatectomy liver failure? *HPB* 18:494-503, 2016
- Clavien PA, Petrowsky H, DeOliveira ML, et al: Strategies for safer liver surgery and partial liver transplantation. *N Engl J Med* 356:1545-1559, 2007
- Gupta M, Choudhury PS, Singh S, et al: Liver functional volumetry by Tc-99m mebrofenin hepatobiliary scintigraphy before major liver resection: A game changer. *Indian J Nucl Med* 33:277-283, 2018
- Dinant S, de Graaf W, Verwer BJ, et al: Risk assessment of posthepatectomy liver failure using hepatobiliary scintigraphy and CT volumetry. *J Nucl Med* 48:685-692, 2007
- Ekman M, Fjälling M, Friman S, et al: Liver uptake function measured by IODIDA clearance rate in liver transplant patients and healthy volunteers. *Nucl Med Commun* 17:235-242, 1996
- Ekman M, Fjälling M, Friman S, et al: Liver uptake function measured by IODIDA clearance rate in liver transplant patients and healthy volunteers. *Nucl Med Commun* 17:235-242, 1996
- Rahbari NN, Garden OJ, et al: Posthepatectomy liver failure: A definition and grading by the International Study Group of Liver Surgery (ISGLS). *Surgery* 149:713-724, 2011
- de Graaf W, van Lienden KP, van den Esschert JW, et al: Increase in future remnant liver function after preoperative portal vein embolization. *Br J Surg* 98:825-834, 2011
- Cieslak KP, Huisman F, Bais T, et al: Future remnant liver function as predictive factor for the hypertrophy response after portal vein embolization. *Surgery* 162:37-47, 2017
- Cieslak KP, Olthof PB, van Lienden KP, et al: Assessment of liver function using (99m)Tc-mebrofenin hepatobiliary scintigraphy in ALPPS (associating liver partition and portal vein ligation for staged hepatectomy). *Case Rep Gastroenterol* 9:353-360, 2015
- Olthof PB, Tomassini F, Huespe PE, et al: Hepatobiliary scintigraphy to evaluate liver function in associating liver partition and portal vein ligation for staged hepatectomy: Liver volume overestimates liver function. *Surgery* 162:775-783, 2017
- Denys A, Prior J, Bize P, et al: Portal vein embolization: What do we know? *CVIR* 35:999-1008, 2012
- van den Esschert JW, de Graaf W, van Lienden KP, et al: Volumetric and functional recovery of the remnant liver after major liver resection with prior portal vein embolization: recovery after PVE and liver resection. *J Gastrointestinal Surg* 13:1464-1469, 2009
- Braat MN, van Erpecum KJ, Zonnenberg BA, et al: Radioembolization-induced liver disease: A systematic review. *Eur J Gastroenterol Hepatol* 29:144-152, 2017
- Braat M, de Jong HW, Seinstra BA, et al: Hepatobiliary scintigraphy may improve radioembolization treatment planning in HCC patients. *EJNMMI Res* 7:2, 2017
- Hogberg J, Rizell M, Hultborn R, et al: Increased absorbed liver dose in Selective Internal Radiation Therapy (SIRT) correlates with increased sphere-cluster frequency and absorbed dose inhomogeneity. *EJNMMI Phys* 2:10, 2015
- Bastiaannet R, Kappadath SC, Kunnen B, et al: The physics of radioembolization. *EJNMMI Phys* 5:22, 2018
- Teo JY, Allen JC Jr., Ng DC, et al: A systematic review of contralateral liver lobe hypertrophy after unilobar selective internal radiation therapy with Y90. *HPB* 18:7-12, 2016
- Teo JY, Allen JC, Ng DC, et al: Prospective study to determine early hypertrophy of the contra-lateral liver lobe after unilobar, Yttrium-90, selective internal radiation therapy in patients with hepatocellular carcinoma. *Surgery* 163:1008-1013, 2018
- Goebel J, Sulke M, Lazik-Palm A, et al: Factors associated with contralateral liver hypertrophy after unilateral radioembolization for hepatocellular carcinoma. *PLoS One* 12:e0181488, 2017
- Lewandowski RJ, Donahue L, Chokechanachaisakul A, et al: (90) Y radiation lobectomy: Outcomes following surgical resection in patients with hepatic tumors and small future liver remnant volumes. *J Surg Oncol* 114:99-105, 2016
- Palard X, Edeline J, Rolland Y, et al: Dosimetric parameters predicting contralateral liver hypertrophy after unilobar radioembolization of hepatocellular carcinoma. *EJNMMI* 45:392-401, 2018
- Orcutt ST, Abuodeh Y, Naghavi A, et al: Kinetic analysis of contralateral liver hypertrophy after radioembolization of primary and metastatic liver tumors. *Surgery* 163:1020-1027, 2018
- Vouche M, Lewandowski RJ, Atassi R, et al: Radiation lobectomy: Time-dependent analysis of future liver remnant volume in unresectable liver cancer as a bridge to resection. *J Hepatol* 59:1029-1036, 2013
- Bouazza F, Poncelet A, Garcia CA, et al: Radioembolisation and portal vein embolization before resection of large hepatocellular carcinoma. *World J Gastroenterol* 21:9666-9670, 2015

39. Olthof PB, Coelen RJS, Bennink RJ, et al: (99m)Tc-mebrofenin hepatobiliary scintigraphy predicts liver failure following major liver resection for perihilar cholangiocarcinoma. *HPB* 19:850-858, 2017
40. Kim YJ, Lee KT, Jo YC, et al: Hepatobiliary scintigraphy for detecting biliary strictures after living donor liver transplantation. *World J Gastroenterol* 17:2626-2631, 2011
41. Engeler CM, Kuni CC, Nakhleh R, et al: Liver transplant rejection and cholestasis: Comparison of technetium 99m-diisopropyl iminodiacetic acid hepatobiliary imaging with liver biopsy. *Eur J Nucl Med* 19:865-870, 1992
42. Nanashima A, Yamaguchi H, Shibasaki S, et al: Relationship between indocyanine green test and technetium-99m galactosyl serum albumin scintigraphy in patients scheduled for hepatectomy: Clinical evaluation and patient outcome. *Hepatol Res* 28:184-190, 2004
43. Nishiyama Y, Yamamoto Y, Hino I, et al: 99mTc galactosyl human serum albumin liver dynamic spect for pre-operative assessment of hepatectomy in relation to percutaneous transhepatic portal embolization. *Nucl Med Commun* 24:809-817, 2003
44. Nanashima A, Tobinaga S, Abo T, et al: Relationship of hepatic functional parameters with changes of functional liver volume using technetium-99m galactosyl serum albumin scintigraphy in patients undergoing preoperative portal vein embolization: A follow-up report. *J Surg Res* 164:e235-e242, 2010
45. Kono Y, Kariya S, Komemushi A, et al: Comparison of Tc-99m GSA scintigraphy and CT volumetry for evaluation in portal vein embolization. *Minimally Invasive Ther Allied Technol* 23:241-246, 2014
46. Haimerl M, Probst U, Poelsterl S, et al: Hepatobiliary MRI: Signal intensity based assessment of liver function correlated to (13)C-Methacetin breath test. *Sci Rep* 8:9078, 2018
47. Geisel D, Ludemann L, Hamm B, et al: Imaging-based liver function tests—past, present and future. *RoFo* 187:863-871, 2015
48. Haimerl M, Verloh N, Zeman F, et al: Gd-EOB-DTPA-enhanced MRI for evaluation of liver function: Comparison between signal-intensity-based indices and T1 relaxometry. *Sci Rep* 7:43347, 2017
49. Geisel D, Raabe P, Ludemann L, et al: Gd-EOB-DTPA-enhanced MRI for monitoring future liver remnant function after portal vein embolization and extended hemihepatectomy: A prospective trial. *Eur Radiol* 27:3080-3087, 2017